ALMA Memo 304:
Relative Sensitivity of Double- and Single-Sideband Systems for both Total Power and Interferometry

A. R. Thompson and L. R. D'Addario

2000-April-22

Abstract. Comparison of double-sideband and single-sideband receiving systems shows that the ratio of sensitivities is proportional to the inverse ratio of the system temperatures. In the case of interferometers, where the complex cross correlation is measured, there is an additional factor of $\sqrt{2}$ by which the sensitivity of double-sideband systems is reduced. This factor, which is not always taken into account, does not apply to total power systems. The relative sensitivity of double- and single-sideband systems is discussed for observations of both continuum and spectral line radiation. The results are then generalized to the intermediate case of unequal sideband gain. Finally, numerical results for ALMA from earlier memos are reviewed and extended.

Dependence of Sensitivity on System Temperature

At millimeter and submillimeter wavelengths it is sometimes possible to obtain better sensitivity for continuum observations with a double-sideband (DSB) receiving system than with a single-sideband (SSB) one. We can compare the performance of these two systems, where both present the same bandwidth at the correlator input, by considering the system temperatures. System temperature is defined as the noise temperature of a broadband (covering both sidebands) thermal source at the input of a hypothetical noise free (but otherwise identical) receiver that would deliver the same available noise power to the correlator or detector. The system temperature thus includes both the antenna noise (resulting from ground radiation and atmospheric attenuation) as well as the receiver noise[†]. (Note that it is also possible to define a narrow-band system temperature that is a function of frequency across the receiver's input bandwidth; our definition gives a gain-weighted average of this quantity, applicable to receivers with any gain ratio between sidebands.) We then define a ratio of the system temperatures as

$$\alpha = \frac{\text{system temperature of double-sideband system}}{\text{system temperature of single-sideband system}}. \tag{1}$$

For total power observation of a weak, continuum source (equal signal in each sideband) with a given integrating time and detector bandwidth, we find:

$$\left[\frac{\text{single-sideband sensitivity}}{\text{double-sideband sensitivity}}\right]_{\text{total power}} = \alpha, \tag{2}$$

where the sensitivity is proportional to the signal-to-noise ratio (SNR) in each case. However, for a two element interferometer, or a cross-correlated antenna pair of an array, again for continuum radiation,

$$\left[\frac{\text{single-sideband sensitivity}}{\text{double-sideband sensitivity}}\right]_{\text{interferometer}} = \sqrt{2}\,\alpha. \tag{3}$$

[†] The system temperatures may be determined at any plane in the signal path. For measurements, the plane just above the receiver's feed horn is often most convenient. However, for astronomical calibration the plane is commonly taken to be above the atmosphere. Since we are discussing only the ratio of two system temperatures, the choice of reference plane has no effect on our results.

The $\sqrt{2}$ factor is not always included in discussions of the relative sensitivity. For example, it is included in discussions in MMA/ALMA Memo 168, which considers interferometry, but not in Memos 170 and 301 which are largely concerned with total power observation. The $\sqrt{2}$ disadvantage of DSB receivers for the interferometer case is recognized in Rogers (1976), and in Thompson, Moran and Swenson (1986) (which we will refer to as TMS). (Note that the relative sensitivities in Table 6.1 of TMS apply to the case $\alpha = 1$.) The difference indicated by Eqs. (2) and (3) results from the fact that the outputs from the two sidebands combine in different ways in the two cases. In the total power case the responses of the two sidebands are scalar quantities (received power), and can be directly added. On the other hand, in interferometry the two responses represent complex visibility and combine as vectors in the complex plane.

So far we have assumed that the SSB system has zero gain in the image sideband, and that the DSB system has equal gain in the two sidebands. Later we will relax these assumptions and allow other sideband ratios.

The $\sqrt{2}$ Factor in Interferometry, Continuum Sources

To obtain the result in Eq. (3) it is necessary to derive the expressions for the outputs of a complex correlator for which the inputs are IF signals from DSB receiving systems. This derivation is given in Chapter 6 of TMS, so here we shall only quote the results [Eqs. (6.16) and (6.18)], which are as follows. For a complex correlator, the real output is

$$(r_d)_{\rm real} = 2|\mathcal{V}||G_{mn}(\Delta\tau)| \cos(2\pi\nu_0\Delta\tau + \phi_{_G}) \cos\big[2\pi\nu_{_{LO}}\tau_g + (\theta_m - \theta_n) - \phi_v\big] \tag{4}$$

and the imaginary output is

$$(r_d)_{\rm imag} = 2|\mathcal{V}||G_{mn}(\Delta\tau)| \sin(2\pi\nu_0\Delta\tau + \phi_{_G}) \cos\big[2\pi\nu_{_{LO}}\tau_g + (\theta_m - \theta_n) - \phi_v\big], \tag{5}$$

where, $|\mathcal{V}|$ is the visibility amplitude, G_{mn} is an instrumental gain term, subscripts m and n refer to the two antennas, $\Delta\tau$ is the delay setting error (geometrical delay minus instrumental delay), ν_0 is the IF center frequency, $\phi_{_G}$ is an instrumental phase term, $\nu_{_{LO}}$ is the local oscillator frequency, τ_g is the geometrical delay, θ_m and θ_n are local oscillator phase terms, and ϕ_v is the visibility phase. In Eqs. (4) and (5) the factor $\cos\big[2\pi\nu_{_{LO}}\tau_g + (\theta_m - \theta_n) - \phi_v\big]$ represents the fringe oscillations. Note that $\nu_0\Delta\tau$ and $\phi_{_G}$ appear in a sine or cosine function that controls the amplitude of the fringes. This result is quite different from the response of a single-sideband system, in which $\nu_0\Delta\tau$ and $\phi_{_G}$ appear as fringe phase terms. If the instrumental delay is adjusted so that $(2\pi\nu_0\Delta\tau + \phi_{_G}) = 0$, the fringe amplitude of the real output is maximized, but the imaginary output becomes zero, that is, it contains only noise. Thus the best DSB sensitivity is obtained by adjusting for this condition and using only the real output. The signal-to-noise ratio from the real output is the same as that from one output of a single-sideband system when the system temperatures are such that $\alpha = 1$. However, in the single-sideband case both the real and imaginary outputs have the same signal-to-noise ratio, and the noise in these outputs is uncorrelated. Thus the overall sensitivity is $\sqrt{2}$ better than that of the double-sideband system.

A useful way of visualizing the responses is shown in Fig. 1, which represents the correlator outputs in the complex plane. The response for an SSB system is shown in Fig. 1a, where the complex visibility vector rotates through one revolution for each fringe cycle. The projections of this vector on the real and imaginary axes represent the two outputs of a complex correlator, which thus contain fringe oscillations in phase quadrature. Figure 1b shows the situation for a DSB system, with the same total levels of signal and noise at the correlator inputs as in Fig. 1a. The two vectors in Fig. 1b rotate in opposite directions: this occurs because a change of phase in the RF signal from the source results in phase changes of opposite sign in the two sidebands. In Fig. 1b, the two vectors cross on the line AB. The point C, which represents the correlator output, oscillates sinusoidally along AB, and produces oscillations in the real and imaginary outputs which are in phase, unlike

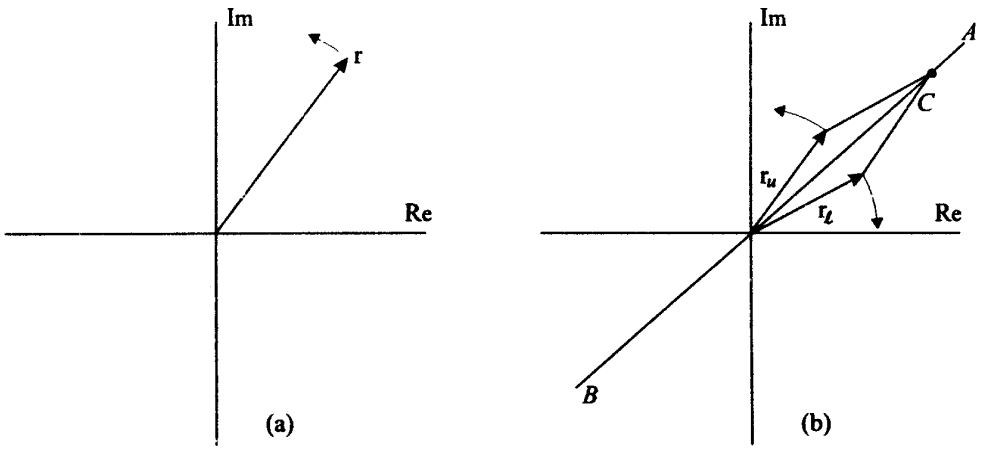

Figure 1 Representation in the complex plane of the output of a correlator with, (a) a single-sideband, and (b) a double-sideband, receiving system. The point C in (b) represents the sum of the upper- and lower-sideband outputs of the correlator.

phase quadrature situation for the single-sideband system. Adjusting the instrumental delay so that $(2\pi\nu_0\Delta\tau + \phi_{_G}) = 0$ causes the line AB to rotate onto the real axis. If the fringes are not stopped, their amplitude and phase can be determined by fitting a sinusoid to the real output. If the fringes are stopped, their amplitude and phase can be measured by periodically making a $\pi/2$ phase shift in the first LO of one antenna (i.e. $\theta_m \rightarrow \theta_m - \pi/2$). With this phase shift the output is given by Eq. (4) with the second cosine function changed to a sine. The value of the expression within the square brackets, which contains the visibility phase, can thereby be determined. Since the time must be divided between the two conditions for the LO phase, the effective averaging time is 1/2 that for an SSB system with a complex correlator.

In the case of the ALMA array, a spectral correlator will be used. In the expression for the correlator response in Eq. (4), the lag delay $\tau_{\rm lag}$ is effectively inserted in series with $\Delta\tau$. Then if the system is adjusted so that $(2\pi\nu_0\Delta\tau + \phi_{_G}) = 0$, Eq. (4) becomes

$$(r_d)_{\rm real} = 2|\mathcal{V}||G_{mn}(\Delta\tau)|\cos(2\pi\nu_0\tau_{\rm lag})\cos\big[2\pi\nu_{_{LO}}\tau_g + (\theta_m - \theta_n) - \phi_v\big]. \qquad (6)$$

Equation (6) shows that, as a function of $\tau_{\rm lag}$, the cross correlation function is real and even. Thus the cross power spectrum, which is the Fourier transform of the cross correlation with respect to $\tau_{\rm lag}$ and frequency, is also real. Like the continuum correlator discussed above, the lag correlator does not provide an imaginary component of the visibility, so the $\sqrt{2}$ factor applies with either one.

Spectral Line Sources

When the signal is in one sideband only, as with a spectral line source, the sensitivity of the SSB system is unaffected but that of the DSB system is reduced by half. This is because the DSB system now has only half as much signal (for the same antenna temperature) but the same amount of noise. For interferometric detection it is now possible to measure both real and imaginary components of visibility simultaneously (just as with an SSB system), so the factor of $\sqrt{2}$ loss discussed in the preceding section does not apply.

The special case in which there are lines of interest in both sidebands is equivalent to the continuum case, both for total power and for interferometry. The proof of this is lengthy, and further discussion can be found in Appendix A.

TABLE 1. (Single-Sideband Sensitivity)/(Double-Sideband Sensitivity) with perfect image rejection

	Total Power	Interferometer
Continuum Source	α	$\sqrt{2}\alpha$
Spectral Line Source	2α	2α

In interferometry, if there are two local oscillators then it is possible to suppress the response to one sideband by producing a frequency offset that affects only one sideband (a technique that is likely to be employed on ALMA). This situation is equivalent to having a spectral line source, even if the actual source emits in the continuum over both sidebands.

Table 1 summarizes all the results so far, covering both line and continuum for both total power and interferometric detection. Recall that this is for pure SSB (zero gain in image band) and pure DSB (equal sideband gains).

Range of α With Ideal Components

To understand the range of system temperature ratios α that might be expected, we now consider some typical implementations, initially with ideal components. We want to examine the sensitivity difference between SSB and DSB systems which are otherwise similar. Therefore, let the SSB system be constructed from a DSB system by the addition a passive, lossless filter between the antenna and the mixer. Consider two cases.

1 If most of the system noise comes from the antenna, i.e. from atmospheric noise or ground radiation, then the double- and single-sideband system temperatures are similar, and $\alpha \to 1$. As Table 1 shows, the SSB system then has a significant advantage in most cases.

2 If most of the system noise comes from the receiver (mixers and IF stages), $\alpha \to \frac{1}{2}$. From Table 1, the two systems are similar in spectral line and the DSB system has an advantage in continuum, due to the extra signal from the second sideband.

In general, α is likely to take a value between $\frac{1}{2}$ and 1. However it is not confined to this range. For example, if noise from the antenna is low but the termination of the image sideband in the single-sideband system is not well cooled and injects a high noise level, then α can be less than $\frac{1}{2}$. Or if the front end is tuned close to the edge of an atmospheric window in such a way that the additional sideband of the double-sideband system falls in a frequency range of enhanced atmospheric noise, then α could be greater than 1.

Now consider adding a low noise amplifier ahead of the mixer and SSB filter. If the amplifier has sufficient gain to make the mixer noise negligible, then $\alpha = 1$ regardless of whether the system noise is dominated by the antenna or receiver. Thus with an amplifier as the input stage, we see that in most of the cases in Table 1 it is advantageous to use an SSB system.

Practical Values of α and Corresponding Relative Sensitivities

In most ALMA front ends at frequencies above 100 GHz the low-noise input stage consists of one or more SIS mixers which are inherently double-sideband devices. To allow only one sideband to be accepted by the front end, two fundamentally different schemes are possible:

- Use of a diplexing filter (or diplexer) which passes only one sideband. To reduce the noise entering through the unwanted (image) sideband the diplexer should be low-loss, and the image band should be terminated in a cold load. If the LO frequency is variable, then the diplexer must be tunable. Examples include Martin-Puplett interferometers and waveguide cavity filters formed by backshorts.
- Use of an image-rejecting mixer, which consists of two mixers operating in phase quadrature with the IF outputs also combined in quadrature. Loads on hybrids and power splitters should be cooled. This type of SSB front end has the advantage that it does not require mechanical tuning. [An application of this technique using SIS mixers is described by Kerr et al. (1998)].

To ensure that the mixer's behavior is unchanged when the SSB components are added, we assume that the mixer sees the same embedding impedance at all significant frequencies in both configurations; that is, we assume that the SSB components are impedance matched. This excludes cavity-type filters which present a reactive impedance in the image sideband.

Consider the first scheme, with a mixer preceded by a matched diplexer, but now let the diplexer be non-ideal. The system temperatures and relative sensitivities then depend upon the following parameters:

- Antenna temperature (sky and spillover) in each sideband
- Receiver temperature (T_R) of the double-sideband receiver
- Ohmic loss of the diplexer
- Physical temperature of the diplexer
- Physical temperature of the image termination
- Sideband rejection factor.

If an image-rejecting mixer is used instead of the diplexer-mixer, with each constituent mixer identical to that of the DSB system, then the situation is exactly equivalent provided that the loss and temperature of the diplexer are replaced by those of the RF hybrid, and the temperature of the image termination is replaced by that of the RF hybrid's termination. We will derive estimates of the realizable range of relative sensitivities for practical values of these parameters.

The sensitivities depend on the signal-to-noise ratios at the input to the correlator or detector. The relative noise of the SSB and DSB systems is described by α, which includes the effects of all the listed parameters. The relative signal depends on the sideband rejection factor, on whether the signal is in both sidebands, and on the detection method. The results are given in Table 1 when the sideband rejection is perfect, but now we wish to consider the non-ideal case. We shall continue to assume that the nominally DSB system has equal gain in the two sidebands. (The gain may vary with intermediate frequency, and the narrow-band noise temperature need not be the same in both sidebands.) For the nominally SSB system, we now take the ratio of the average power gain in the image band to that in the signal band to be $0 \leq \rho \leq 1$. For interferometry, we assume that the instrumental phase is the same in each sideband. The generalization of Table 1 for these conditions is given in Table 2. The proof of this will be omitted here, although some further explanation is given in Appendix A.

Previous Work

Three previous memoranda have considered practical values of antenna and receiver temperatures, taking into account data on the atmospheric opacity at the ALMA site.

Thompson and Kerr (1997, MMA Memo 168) considered only interferometric detection, and they assumed an ideal diplexer with 5K image termination for the SSB receiver, using a DSB mixer

TABLE 2. (Single-Sideband Sensitivity)/(Double-Sideband Sensitivity)

	Total Power	Interferometer
Continuum Source	α	$\frac{\sqrt{2(1+\rho^2)}}{1+\rho}\alpha$
Spectral Line Source	$\frac{2}{(1+\rho)}\alpha$	$\frac{2}{(1+\rho)}\alpha$

TABLE 3. Values of α Derived in Three Memoranda

	225 GHz	650 GHz	950 GHz
MMA 168	0.56–0.61	0.65–0.72	–
MMA 170	0.612	0.784	0.775
ALMA 301	–	0.611–0.725	0.605–0.715

with DSB receiver temperatures of $2hf/k$ and $4hf/k$ for frequency f. They considered frequencies of 225 and 650 GHz, using both first and third quartile measured atmospheric opacities at zenith.

Jewell and Mangum (1997, MMA Memo 170) considered mainly total power detection. They assumed ideal diplexers with 4.2K image termination, using a DSB mixer with a DSB receiver temperature of $2hf/k$. They considered the whole frequency range from <10 to 1000 GHz, using atmospheric opacity from a model corresponding to 1 mm of water at zenith angle 45 deg. Only the line case was discussed.

Lamb (2000, ALMA Memo 301) considered non-ideal diplexers with losses of 0 and 10% and sideband rejections of 0 and 0.1. Physical temperatures of 5 to 295K were used. The DSB receiver temperature without diplexer was varied from $2hf/k$ to $5hf/k$. The atmospheric opacity corresponded to 1 mm of water at zenith angle 40 deg. However, only frequencies of 650 and 950 GHz were included. Only the line case was discussed.

It can thus be seen that the various memos used similar, but not identical, atmospheric opacity; different receiver temperatures; and different frequencies. Lamb considered the widest range of parameters, except for frequency where he covered only the highest bands.

Thompson and Kerr (1997) give estimates of α in their Tables 1–3. In Jewell and Mangum (1997), Figure 4 is a plot of $(2\alpha)^2$ vs. frequency. In Lamb (2000), Figures 3 and 4 are plots of $\Gamma = 2\alpha/(1+\rho)$ vs. receiver temperature; in his notation, $R = 1/\rho$. By combining these results in a consistent manner, we obtain the estimates of Table 3. We deleted parameter ranges that we find impractical by considering only receiver temperatures greater than $3hf/k$ and ignoring cases with room-temperature components in ALMA 301; including receiver temperature $4hf/k$ and not $2hf/k$ from MMA 168; and selecting frequencies from MMA 170 that are common with the other memos. There is reasonably good agreement among the memos. MMA 170 tends to give higher values of α because the receiver temperature was taken to be lower, $2hf/k$.

Numerical Results

From the relative sensitivity factors in Table 2 and the ranges of α in Table 3, we obtain numerical estimates of the sensitivity ratio. These are given in Table 4.

TABLE 4. Values of (SSB Sensitivity)/(DSB Sensitivity)

	225 GHz	650 GHz	950 GHz
Total Power			
Continuum	0.56–0.61	0.61–0.78	0.61–0.78
Line, $\rho = 0$	1.12–1.22	1.22–1.56	1.21–1.56
Line, $\rho = 0.1$	1.02–1.11	1.11–1.42	1.10–1.42
Interferometer			
Continuum, $\rho = 0$	0.79–0.86	0.86–1.10	0.86–1.10
Continuum, $\rho = 0.1$	0.72–0.79	0.79–1.01	0.78–1.01
Line, $\rho = 0$	1.12–1.22	1.22–1.56	1.21–1.56
Line, $\rho = 0.1$	1.02–1.11	1.11–1.42	1.10–1.42

Notes: When observing spectral lines in both sidebands, the results are the same as for continuum. Interferometric observations with one sideband suppressed via a frequency offset correspond to the spectral line case, even for a continuum source.

Discussion

For the most part, Table 4 shows that DSB provides better sensitivity for continuum sources and SSB provides better sensitivity for line sources. The SSB advantage is greatest at the highest frequencies, where the atmospheric opacity is worst. It is also greatest at the lowest receiver temperatures, and does not exceed 33% if the DSB receiver temperature is $5hf/k$, even with an ideal diplexer.

The choice of SSB or DSB for the front ends of ALMA requires consideration not only of the relative sensitivities estimated here, but also of practical matters like system complexity, manufacturability, and maintainability. Some discussion of these issues is given in Lamb (2000).

Appendix A: DSB SIGNAL PROCESSING STRATEGIES IN INTERFEROMETRY

As shown in the text, an interferometer with purely DSB receivers cannot simultaneously measure the real and imaginary parts of the visibility of a continuum source. By using $\pi/2$ phase switching in the first LO and by adjusting the delay and instrumental gain for maximum SNR, we obtain measurements of the real and imaginary parts separately at the different switch positions, using a single real correlator. (Alternatively, the complex visibility can be obtained by letting the fringes run and fitting a sine wave to the single correlator output; the signal-to-noise ratio will be the same.) On the other hand, with purely SSB receivers we can measure both parts simultaneously by using two correlators, one of which has a $\pi/2$ phase shift (Hilbert transform) in one signal path; this setup is sometimes called a "complex correlator." This leads to the $\sqrt{2}$ factor in sensitivity between SSB and DSB, provided that the broadband system temperature (as defined in the text) is the same for both.

Now consider the more general situation where the receivers have a power gain ratio of $0 < \rho < 1$ between one sideband ("image") and the other ("signal"). We assume that the receivers of the two antennas are identical, and that ρ is known by *a priori* calibration. If we again provide for phase switching in the first LO but also implement a complex correlator, it is possible to achieve optimum detection for any value of ρ. The result is a linear combination of the measurements made in the two positions of the phase switch, where the weighting depends on ρ. Assuming that the complex visibility is the same in both sidebands (continuum source), and that the instrumental phase is the

same in both (ρ is real), we can represent the complex correlator output with zero phase shift of the local oscillator as $C_0 = G_{mn}(\mathcal{V} + \rho\mathcal{V}^*)$, and with the $\pi/2$ phase shift as $C_{\pi/2} = G_{mn}(j\mathcal{V} - j\rho\mathcal{V}^*)$. Here G_{mn} is the gain in the signal sideband, so ρG_{mn} is the gain in the image sideband; j is the unit imaginary number; and $*$ denotes complex conjugate. Note that in the expression for $C_{\pi/2}$ the j factors have opposite signs for the two sidebands, because the $\pi/2$ phase shift causes the corresponding vectors in the complex plane to rotate through $\pi/2$ in opposite directions. The optimum estimate of the visibility, $\hat{\mathcal{V}}$, is then found to be

$$2G_{mn}\hat{\mathcal{V}} = \frac{1}{1+\rho^2}(C_0 - jC_{\pi/2}) + \frac{\rho}{1+\rho^2}(C_0 + jC_{\pi/2})^*. \tag{A1}$$

This result holds regardless of the power spectrum of the system noise, which might be stronger in one sideband than the other, because the noise at the correlator input depends only on the total. Under our definition of system temperature $T_{\rm sys}$, the total noise power delivered to the correlator is proportional to $T_{\rm sys}|G_{mn}|(1+\rho)$. Assuming that equal time is spent in each phase switch position, each correlation will have the same standard deviation due to the noise, and the two will be weighted as shown in (A1). After some additional algebra, this results in a standard deviation of $\hat{\mathcal{V}}$ proportional to

$$\frac{1+\rho}{\sqrt{1+\rho^2}}T_{\rm sys}. \tag{A2}$$

From (A2) it can be seen that the DSB ($\rho = 1$) variance is $\sqrt{2}$ larger than the SSB ($\rho = 0$) variance, in agreement with the result in the Table 1. Expression (A2) is the basis of the more general result given in Table 2.

The weighting in (A1) can be understood as follows. Each major term is the response for one sideband, so that the two have been separated. For DSB ($\rho = 1$), each major term has the same weighting, which causes the imaginary parts of C_0 and $C_{\pi/2}$ to cancel. Those terms are ignored because they contain only noise; the real part of $\mathcal{V}$ is measured half the time and the imaginary part is measured the other half, as explained earlier. Alternatively, this could be viewed as averaging the two sidebands, each of which gives an equally accurate measure of the complex visibility. For SSB ($\rho = 0$), the second major term has zero weight because it represents the measurement of the image sideband, which then contains only noise.

The special case of line sources in both sidebands is seen to be equivalent if the two terms of (A1) are kept separate. When $\rho = 1$ (DSB), the sensitivity in each sideband is $\sqrt{2}$ worse than for a continuum source of the same antenna temperature, since we are unable to average the two sidebands. When $\rho = 0$ (SSB), we can observe the two lines sequentially by retuning the LO; in the same total time, the sensitivity is again $\sqrt{2}$ worse. So the ratio of the SSB to DSB sensitivity remains as calculated here for continuum. Similar arguments can be made for total power detection.

REFERENCES

Jewell, P. R. and J. G. Mangum, System temperatures, Single Versus Double Sideband Operation, and Optimum Receiver Performance, *MMA Memo 170*, NRAO, Socorro, 1997. Also in *Int. J. of Infrared & Millimeter Waves*, Vol. 20, No. 2, Feb 1999.

Kerr, A. R., S.-K. Pan, and H. G. LeDuc, An Integrated Sideband Separating SIS Mixer for 200-280 GHz, *Proceedings of the Ninth International Symposium on Space Terahertz Technology, 17-19 March 1998*, pp. 215–221. Also distributed as MMA Memo 206, 1998.

Lamb, J. W., SSB vs. DSB for Submillimeter Receivers, *ALMA Memo 301*, NRAO, Socorro, 2000.

Rogers, A. E. E., Interferometers and Arrays, in *Methods of Experimental Physics*, Vol. 12, Part C, M. L. Meeks, Ed., Academic Press, New York, 1976, pp. 139–157.

Thompson, A. R. and A. R. Kerr, Relative Sensitivities of Single and Double Sideband Receivers for the MMA, *MMA Memo 168*, NRAO, Socorro, 1997.

Thompson, A. R., J. M. Moran, and G. W. Swenson, Jr., *Interferometry and Synthesis in Radio Astronomy*, Wiley, New York, 1986, Reprinted by Krieger, Malabar, FL.